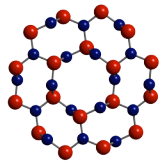

Electronic and Optical Excitations in Noble Metal Clusters and Si Nanoshells

Serdar Öğüt

Department of Physics, University of Illinois at Chicago

Outline

- Silver and Gold Clusters (Structures, Polarizabilities)
- Optical Properties within TDLDA
- TDLDA vs GWBSE
- Quasiparticle Gaps in Si Nanoshells
- Exciton Coulomb Energies in Si Nanoshells

Supported by DOE under Grant No DE-FG02-03ER15488

Collaborators

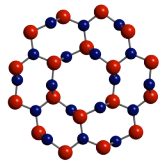

- Juan Carlos Idrobo (UIC, Vanderbilt, ORNL)
- Kopinjol Baishya (UIC)
- Weronika Walkosz (UIC)
- Kimberly Frey (UIC)
- Shing Fan Yip (UIC, UW Madison)

- Julius Jellinek, Jinlan Wang, Karoly Nementh (Argonne)
- Koblar A. Jackson, Mingli Yang (Central Michigan)

- Murilo Tiago (ORNL)
- Fernando Reboredo (ORNL)

Introduction

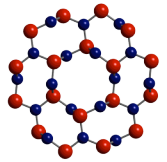

- Due to their intriguing physical/chemical properties (of particular relevance in catalysis, optoelectronics, and nanophotonics applications), noble metal (Cu, Ag, Au) clusters and nanoparticles, currently a topic of technological and fundamental interest.

- Electronic configuration: $nd^{10}(n+1)s^1p^0$. Though completely filled, molecular orbitals associated with *d* electrons have close energetic proximity to and spatial overlap with *sp* states, giving rise to important structural, electronic, and optical properties.

- One particular area, posing a computational challenge is related to accurate modeling of optical properties of noble metal clusters.

- As an example, measured spectra for Ag_n ($n < 40$) embedded in rare-gas matrices have been available since the early 1990s, but direct comparisons with *ab initio* modeling techniques have lagged significantly.

- Recent results from extensive searches yielded ground state and low-energy isomers (up to $n = 20$) ⇨ Use them to compute absorption spectra for comparison with experiment and to investigate the role of *d* electrons on the spectra.

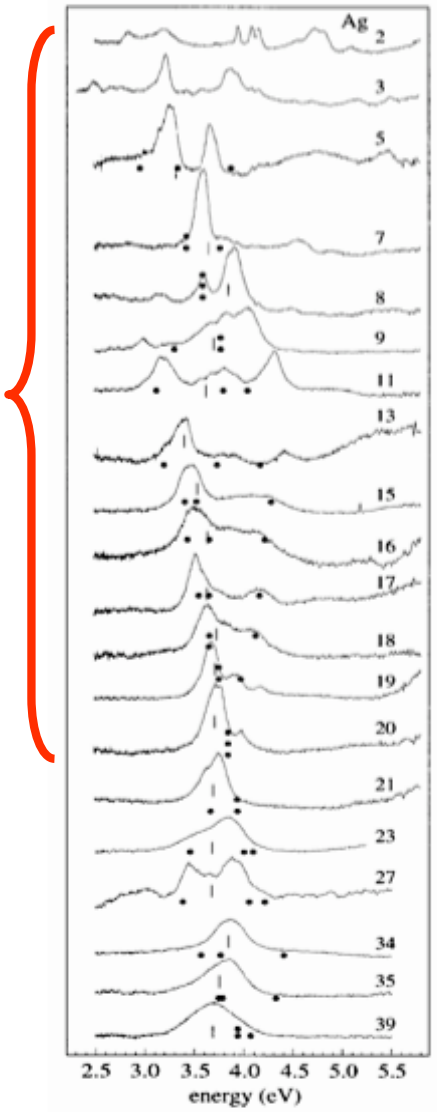

W. Harbich, Phil. Mag. B 79, 1307 (1999)

Motivation (Computational Challenge)

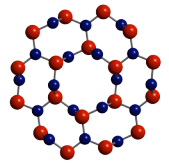

- Two of the state-of-the-art computational techniques for calculating optical excitations in materials: Time-dependent linear response theory using DFT (TDDFT) and adiabatic LDA (TDLDA), and Green's function many-body perturbation methods such as GW+Bethe-Salpeter Equation (GWBSE).

- Computational demand for TDLDA (2-point kernel) considerably smaller compared to GWBSE (4-point kernel). GWBSE, however, gives much more accurate excitation energies in extended systems (excitonic effects).

- The two methods mostly applied to *sp*-bonded clusters with considerable success. Systematic application and comparison of TDLDA and GWBSE in finite systems with tightly bound *d* electrons to investigate the role of *d* electrons in optical excitations.

Calculated Ground State Structures, Au_n (n = 3-14,20)

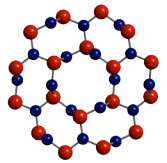

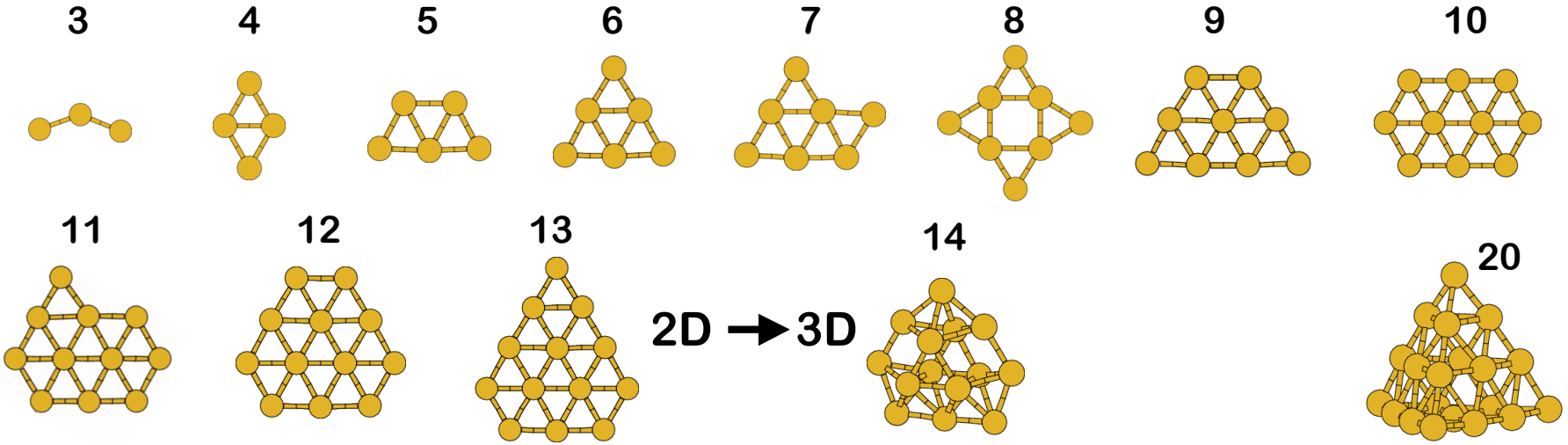

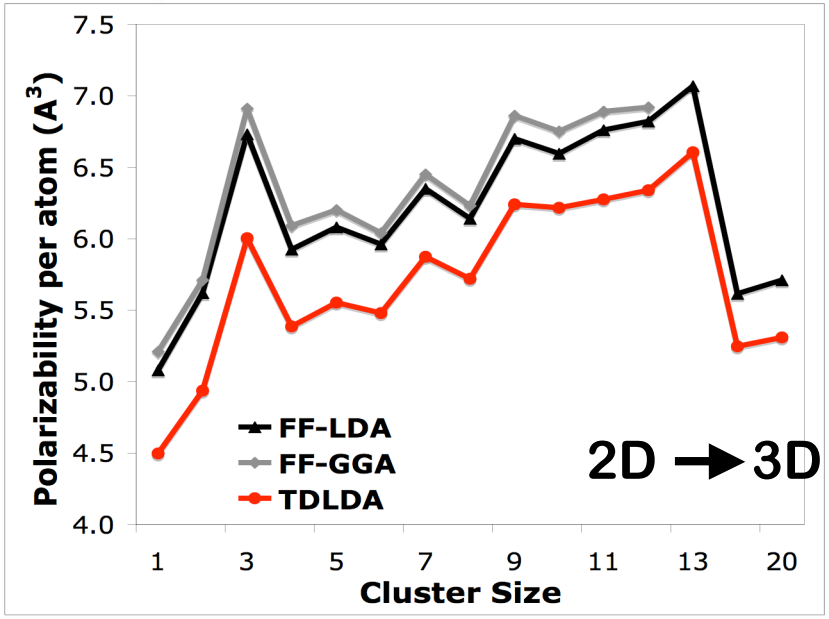

- For Au clusters, shape transition from 2D to 3D at n = 14 (Ag clusters at n = 7).
- Significant drop in the static polarizability correlates with this shape transition.

Calculated Ground State Structures, Ag_n (n = 10-20)

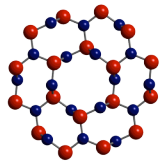

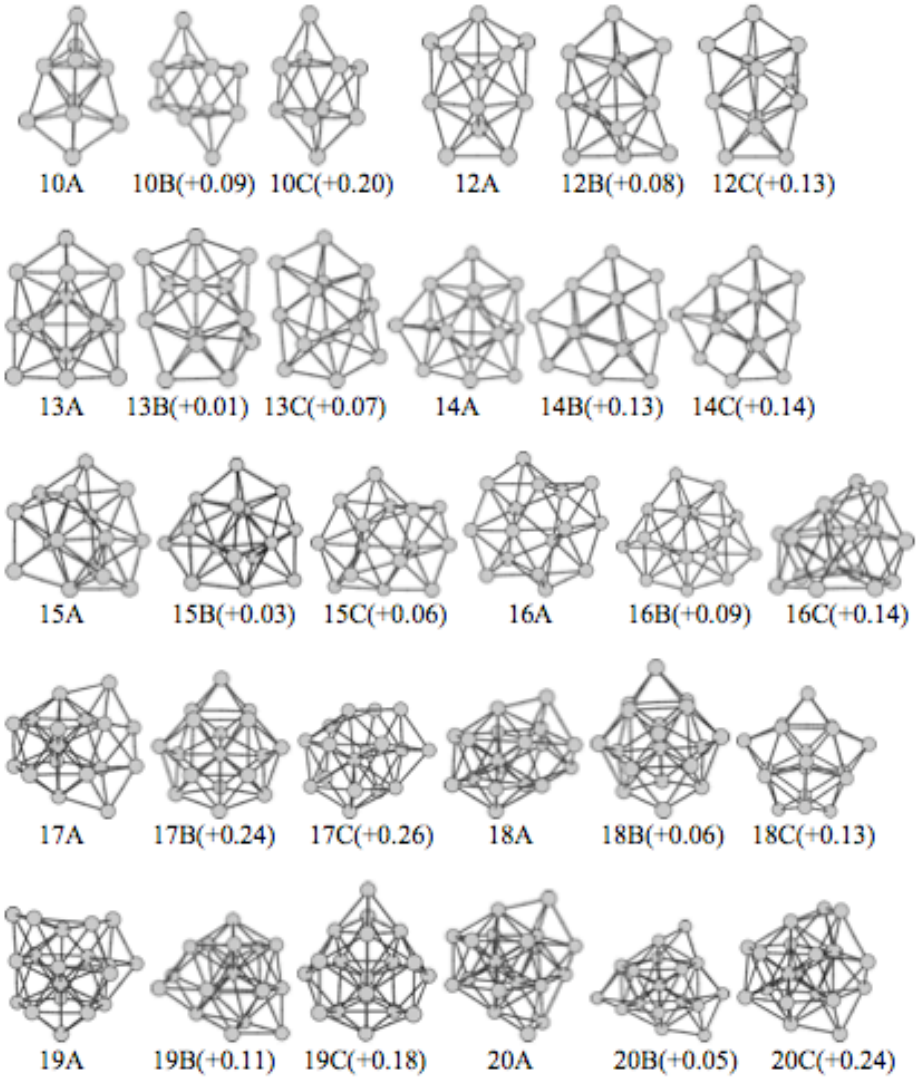

- **Many low-energy isomers at a given size.**
- **Close-packed structures, high coordination numbers.**
- **Shape evolution (from layered prolate to oblate to spherical).**

TDLDA Linear Response

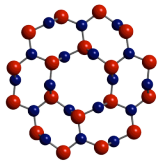

Polarizability: $\delta\rho(\mathbf{r},E) = \int d\mathbf{r}'\, \Pi(\mathbf{r},\mathbf{r}',E) V_{ext}(\mathbf{r}',E)$

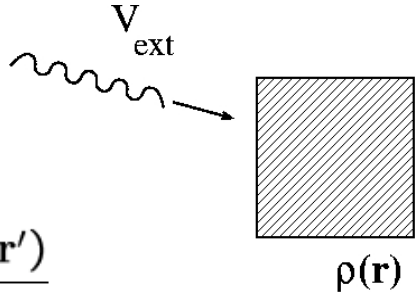

Expansion in poles:

$$\Pi(\mathbf{r},\mathbf{r}',E) = \sum_m \frac{\rho_m^\star(\mathbf{r})\rho_m(\mathbf{r}')}{E-\omega_m} - \sum_m \frac{\rho_m(\mathbf{r})\rho_m^\star(\mathbf{r}')}{E+\omega_m}$$

Eigenvalue problem:

$$\sum_{v'c'} \left[(\varepsilon_c-\varepsilon_v)^2\delta_{cc'}\delta_{vv'} + 2\sqrt{\varepsilon_c-\varepsilon_v}K^{LDA}_{vc,v'c'}\sqrt{\varepsilon_{c'}-\varepsilon_{v'}}\right] F^m_{v'c'} = \omega_m^2 F^m_{vc}$$

$$\rho_m(\mathbf{r}) = \sum_{vc}\sqrt{\frac{\varepsilon_c-\varepsilon_v}{\omega_m}}F^m_{vc}u_v(\mathbf{r})u_c(\mathbf{r})$$

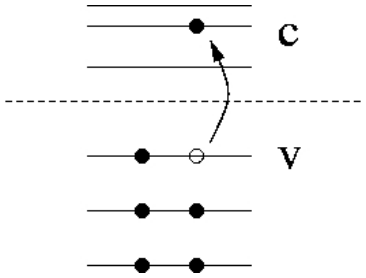

$$K^{LDA}_{vc,v'c'} \equiv \int d\mathbf{r}d\mathbf{r}' u_v(\mathbf{r})u_c^\star(\mathbf{r})K^{LDA}(\mathbf{r},\mathbf{r}')u_{v'}^\star(\mathbf{r}')u_{c'}(\mathbf{r}')$$

$$K^{LDA} = V_{Coul} + f_{xc} \qquad f_{xc} = \left.\frac{\delta V_{xc}}{\delta\rho}\right|_{LDA}$$

Frequency representation: M. Casida (1995)

Comparison with Experiment

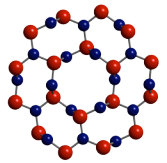

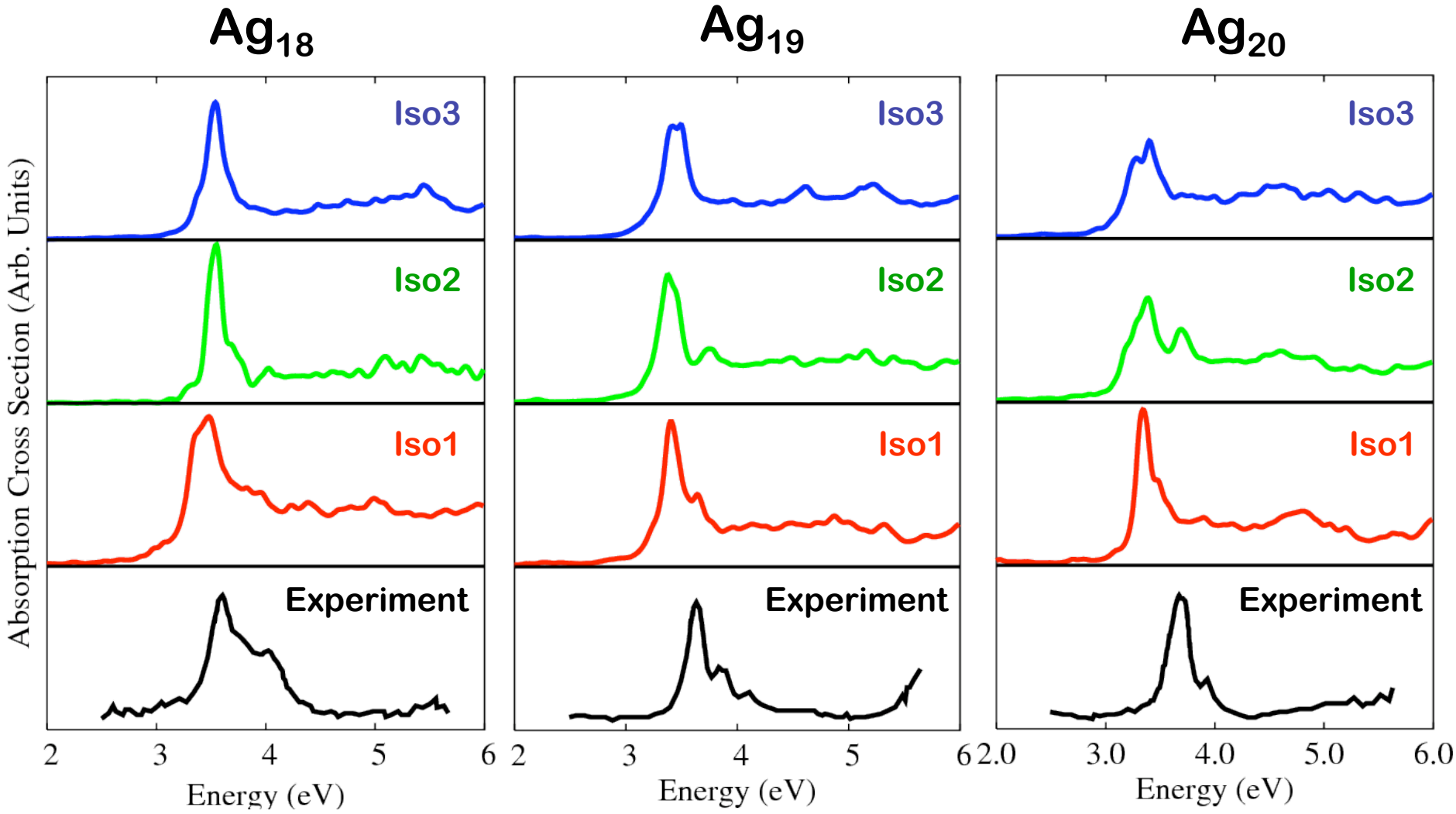

Integrated Oscillator Strengths

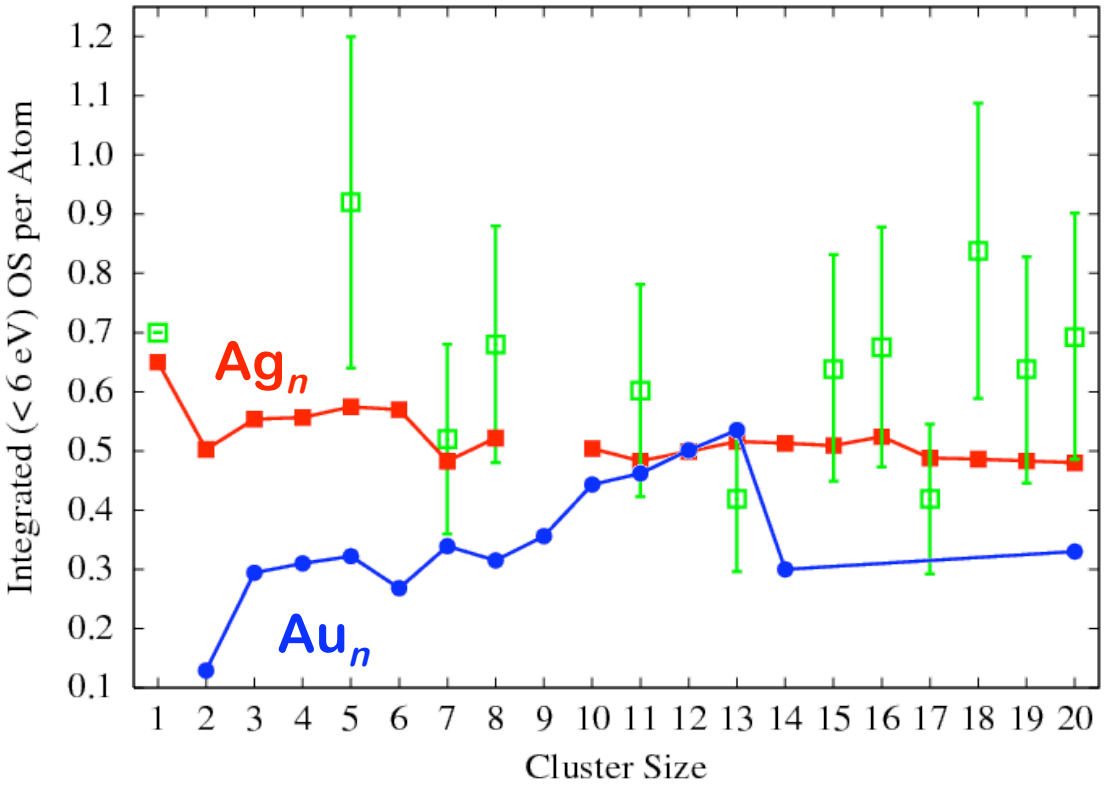

- Screening by *d* electrons quenches the OS in noble metal clusters.
- Integrated OS (below 6 eV) per *s* electron significantly below 1.
- Generally good agreement with experimental data.
- *d* electron screening more enhanced in Au_n clusters.

d-character of Low-energy Excitations

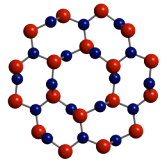

To understand the effect of *d* states on the OS more quantitatively, calculated the % *d* character for transitions below E_{cut} = 6 eV

$$\%d = \frac{\sum_{n}^{\Omega_n < E_{cut}} f_n \sum_{vc} |F_{vc}^{n}|^2 |\langle d | \phi_v \rangle|^2}{\sum_{n}^{\Omega_n < E_{cut}} f_n}$$

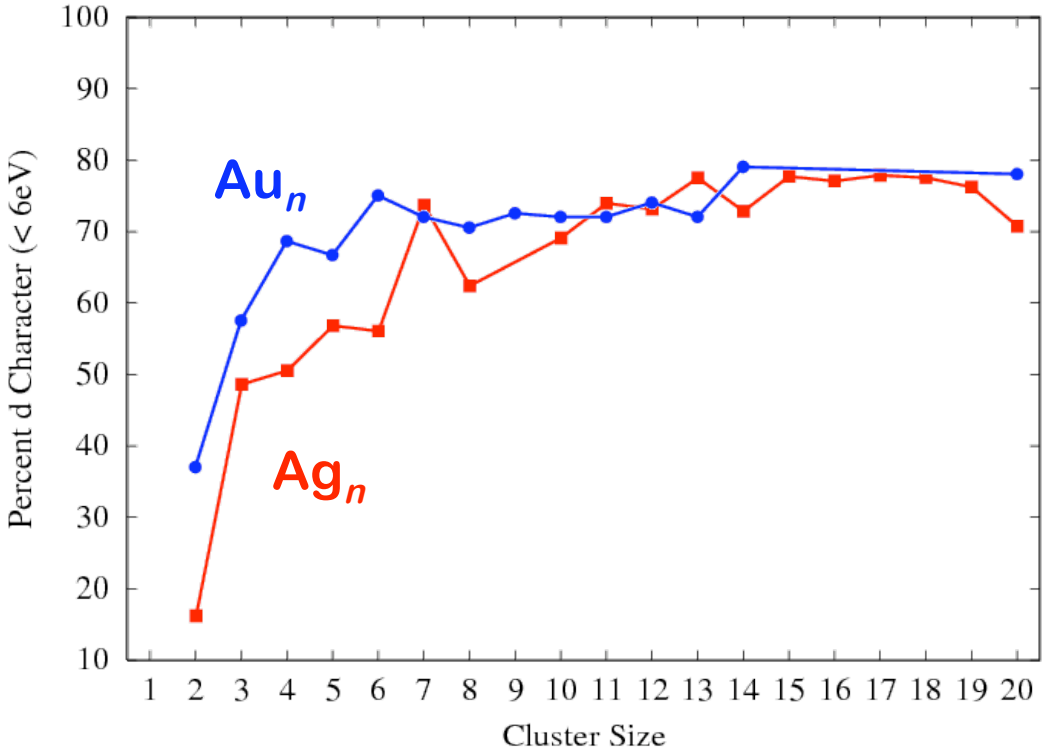

- ***d*** **contribution below 6 eV increases almost monotonically up to *n* ~ 13 with cluster size.**

- **For larger clusters, most of the low energy transitions (about 70%) originate from *d* levels.**

- ***d*** **character in Au$_n$ larger than in Ag$_n$ due to enhanced *sd* hybridization.**

Comparison with Mie-Gans Theory

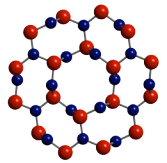

$$\sigma_{abs}(\omega) = \frac{4\pi\omega ABC}{9c} \sum_{i=1}^{3} \frac{\varepsilon_2(\omega)}{\left[G_i(\varepsilon_1(\omega) - \varepsilon_m) + \varepsilon_m\right]^2 + \left[G_i\varepsilon_2(\omega)\right]^2}$$

Prolate

$A = B < C$

$G_1 = G_2 > G_3$

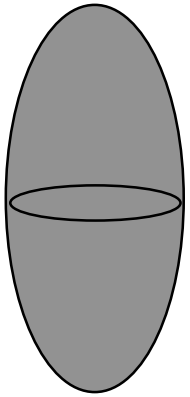

Sphere

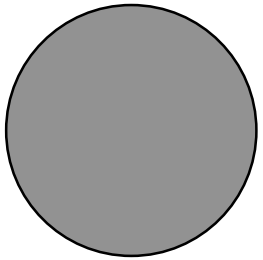

$A = B = C$

$G_1 = G_2 = G_3 = 1/3$

Oblate

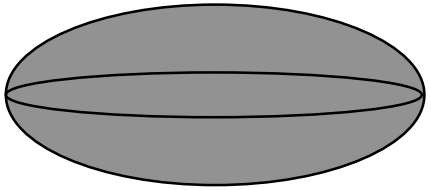

$A = B > C$

$G_1 = G_2 < G_3$

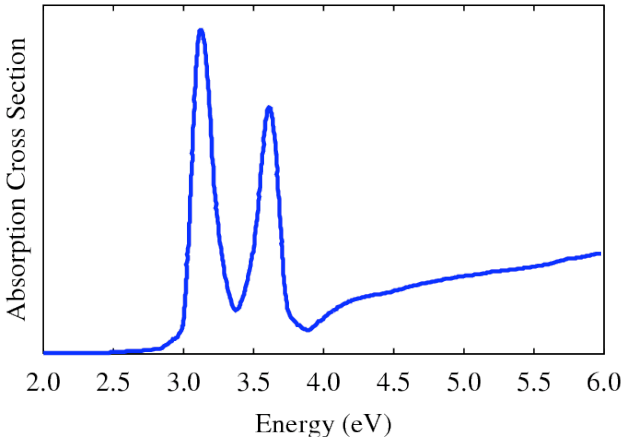

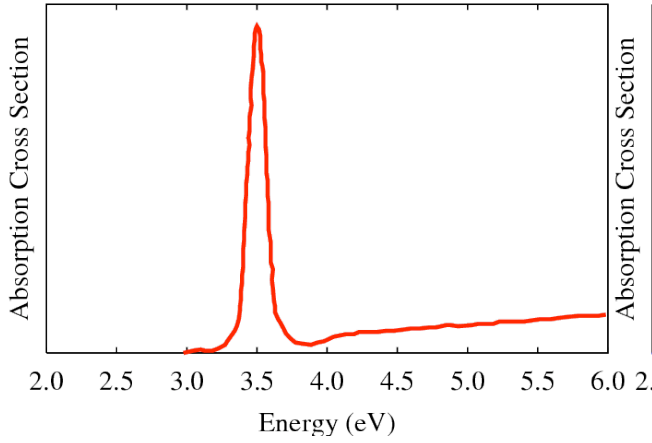

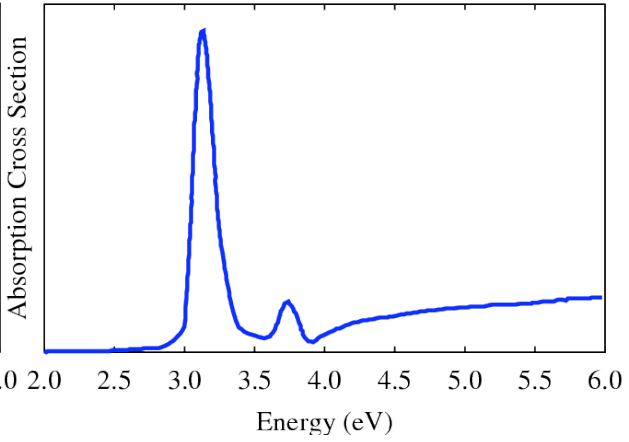

Comparison with Mie-Gans Theory

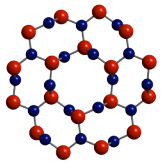

Calculated normalized moments of inertia

$$\langle I_i \rangle = \frac{3I_i}{I_1 + I_2 + I_3}$$

to determine the shape of clusters

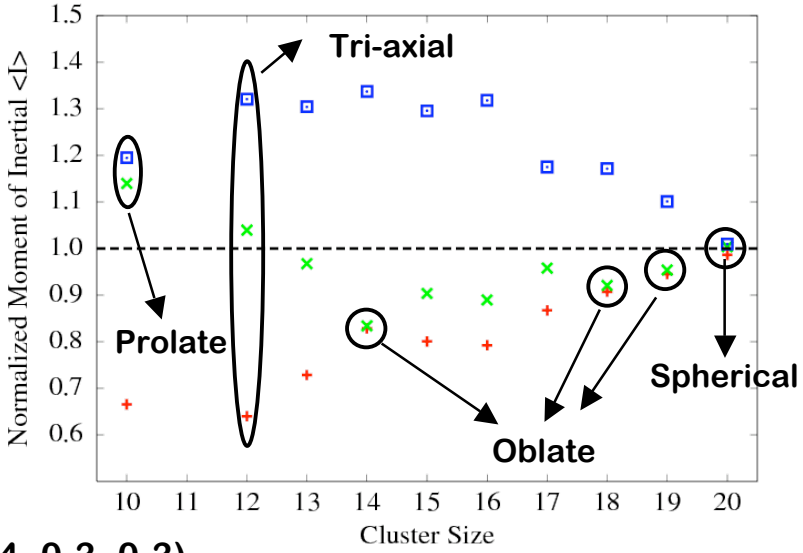

(0.45, 0.35, 0.2)

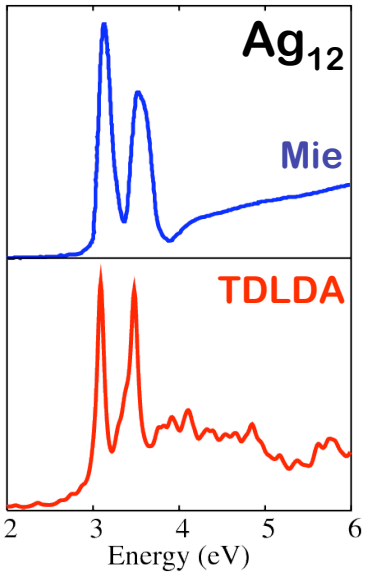

(0.6, 0.2, 0.2)

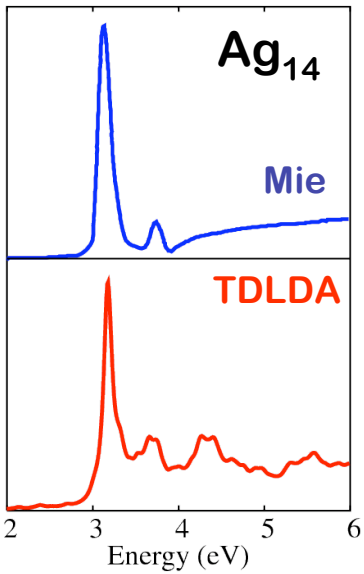

(0.4, 0.3, 0.3)

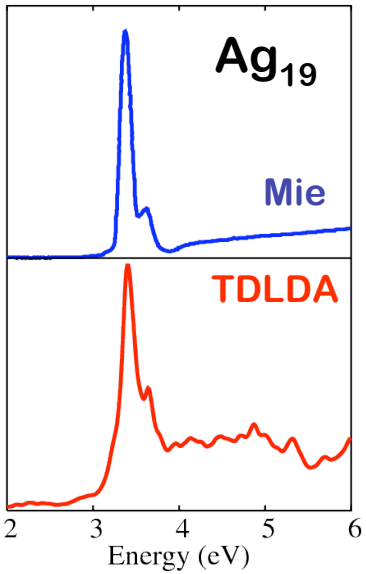

(1/3, 1/3, 1/3)

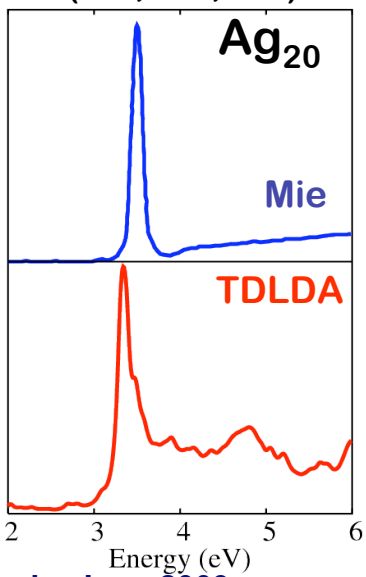

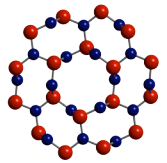

Electronic Excitations: GW theory

$$\Sigma = i\,GW\Gamma_{LDA}$$

$$W = V_{coul} + V_{coul}PW$$
$$= V_{coul} + V_{coul}\Pi_{LDA}V_{coul}$$

- Electron screening from time-dependent DFT-LDA.
- Explicit energy integration.
- LDA vertex included in Self-Energy.
- Results directly comparable to photoelectron spectroscopy.

Bethe-Salpeter Equation

Many-body neutral excitations: $|S\rangle = \sum_{vc} A^S_{vc}|vc\rangle + corrections$

Eigenvalue problem: $(\varepsilon^{qp}_c - \varepsilon^{qp}_v)\,A^S_{cv} + \sum_{c'v'}\langle vc|K^{BSE}|c'v'\rangle A^S_{c'v'} = \Omega^S A^S_{cv}$

$$K^{BSE} = -i\,[V + W + V\sqcap f_{xc}]$$

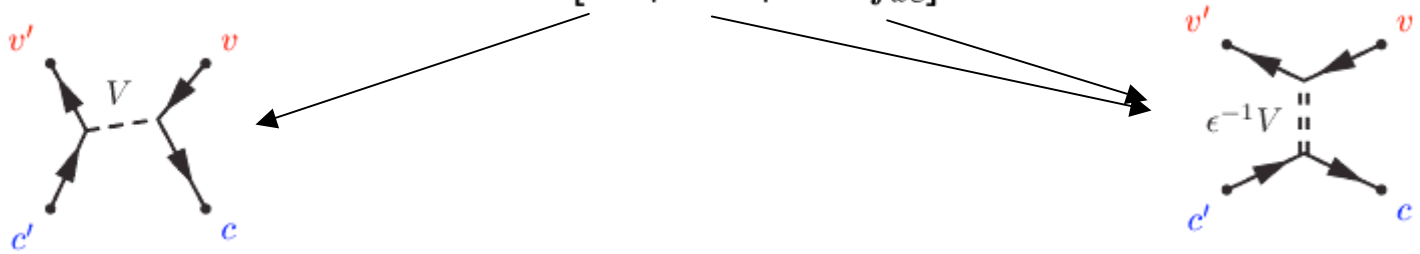

Electronic Excitations (IP and EA) Comparison with ΔSCF and Experiment

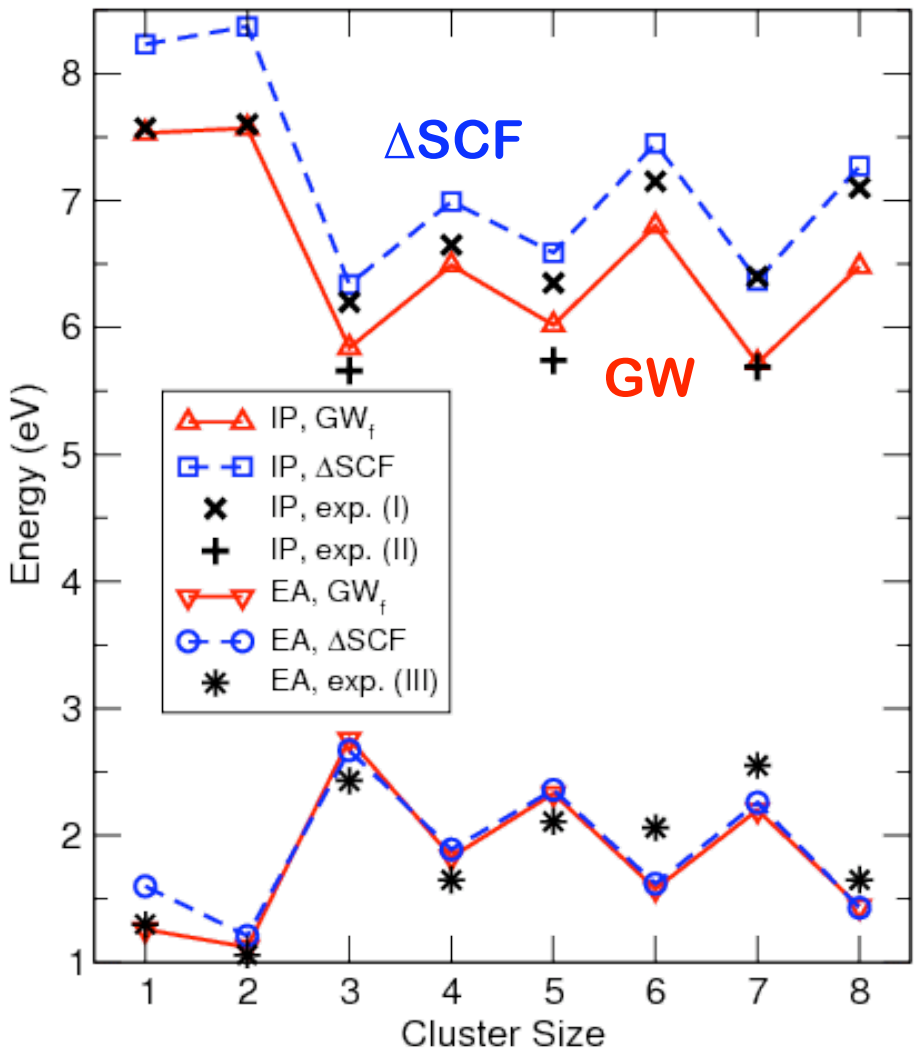

- Within ΔSCF *IP = E(n-1) - E(n)* and *EA = E(n) - E(n+1).*
- Within GW *IP = - HOMO* and *EA = - LUMO.*

- Generally quite good agreement of GW results with experiment (especially Ag and Ag_2). Agreement not so good with ΔSCF.
- Σ very sensitive to the number of virtual orbitals. Convergence accelerated by including a *static remainder* (estimate the numerical error by truncating the sum over virtual orbitals at the level of COHSEX).

	IP (eV)			EA (eV)		
	NS	ST	Exp	NS	ST	Exp
Ag	7.12	**7.53**	**7.57**	0.92	**1.26**	**1.30**
Ag_2	6.27	**7.54**	**7.60**	0.82	**1.12**	**1.06**

(700 orbitals included in Σ)

Electronic Excitations: Case of Ag^+

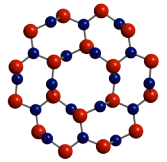

- Observed good agreement at this level of theory due to the fact that HOMO and LUMO of Ag_n ($n \leq 8$) have almost entirely *sp* character (little or no *d* character). For example, in Ag_2, HOMO is 92% *sp*, 8 % *d*, LUMO is 98 % *sp*, and 2% *d*.

- Singly ionized Ag atom, Ag^+, is a good test case for a system with large (entirely) *d* character in HOMO (and purely *s* character in LUMO!). IP of Ag^+ is the double IP of Ag, which is experimentally available. EA of Ag^+ is the IP of neutral Ag!

	IP (eV)			EA (eV)		
	NS	ST	Exp	NS	ST	Exp
Ag^+	16.64	**18.92**	**21.50**	7.34	**7.64**	**7.57**

- 2.6 eV underestimate of IP in Ag^+ (4*d* level) due to core-valence separation in the pseudopotential construction (standard $4d^{10}5s^15p^0$ reference). Though 4*s* and 4*p* levels are ~ 80 and 50 eV below the 4*d* level, due to their strong *spatial* overlap with 4*d* levels, exchange and correlation among 4*s*, 4*p*, and 4*d* electrons are not described properly by a Slater type exchange-correlation [Rohlfing et al. PRL 75, (1995)]

- Remedy: Create semi-core pseudopotentials by keeping 4*s* and 4*p* levels in the valence. Use the reference $4s^24p^64d^{10}$ with *sp* core radii ~ 1.1 a.u. Very deep pseudopotentials. Use $h = 0.2$ a.u (limited tests)

	NS	ST	Exp	NS	ST	Exp
Ag^+(semicore)	20.67	**21.85**	**21.50**	7.04	**7.30**	**7.57**

Optical Excitations within GWBSE and TDDFT: Ag and Ag_2

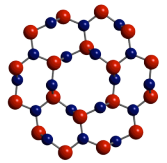

Ag

	TDLDA	GWBSE	Experiment
5s → 5p	4.09	3.68	3.74
5s → 6p	5.44	6.05	6.01

Ag_2

	TDLDA	GWBSE	Experiment
A - X	3.11	2.54	2.85
B - X	3.96	3.99	4.44
C - X	4.75	4.27	4.67

GWBSE clearly performs well for Ag atom. In Ag_2, agreement with experiment not as good. TDLDA in slightly better agreement (perhaps).

Optical Excitations within GWBSE and TDDFT & Comparison with Experiment

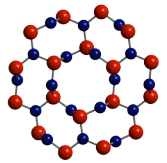

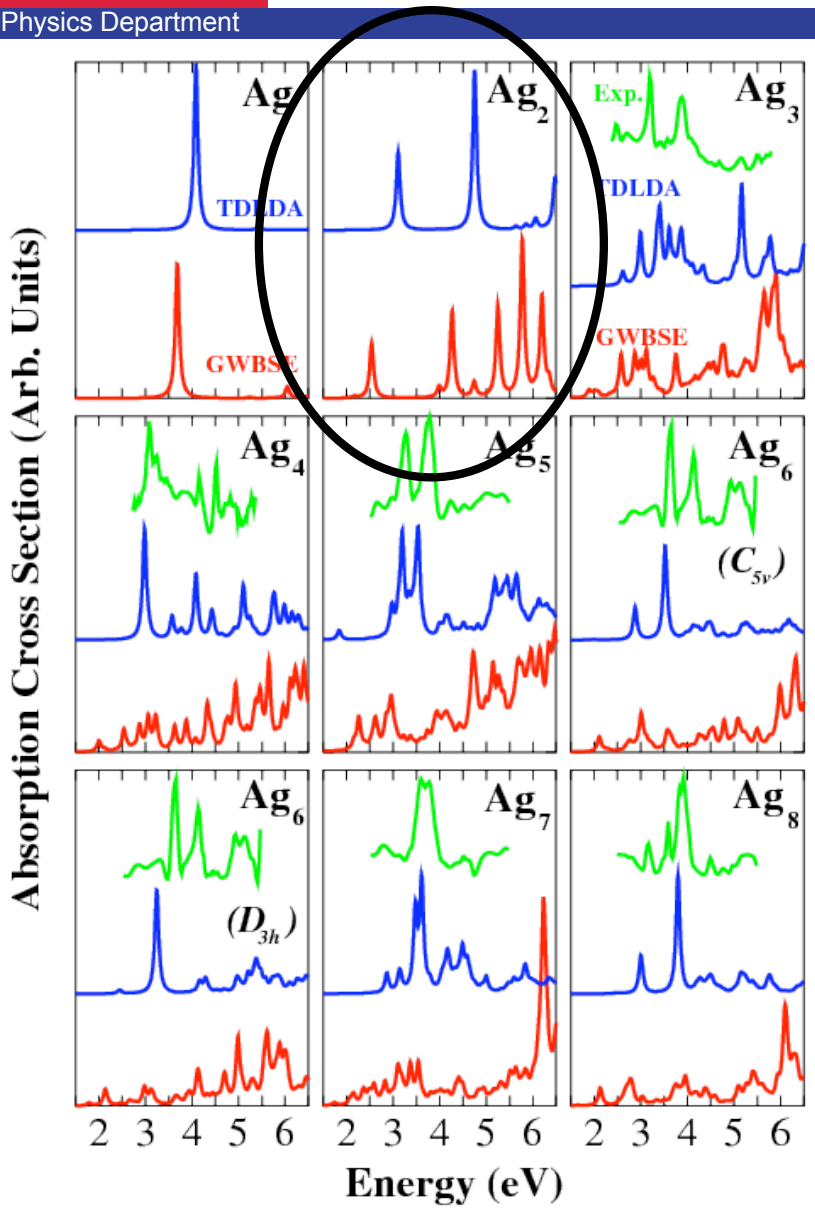

- For n >2, agreement between TDLDA and GWBSE very poor. At low energies, OS from GWBSE quenched significantly, above 5 eV, high OS transitions.

- TDLDA has clearly better agreement with experimental data (esp. $n = 5 - 8$).

- Exchange-correlation effects involving 4*d* orbitals and strong non-locality of the BSE kernel are the main reasons for this behavior.

- Even a small mixture of *d* character results in significant quenching and red-shifting of the predicted transitions at the GWBSE level, as best illustrated for the case of Ag_2

Case Study: Ag_2

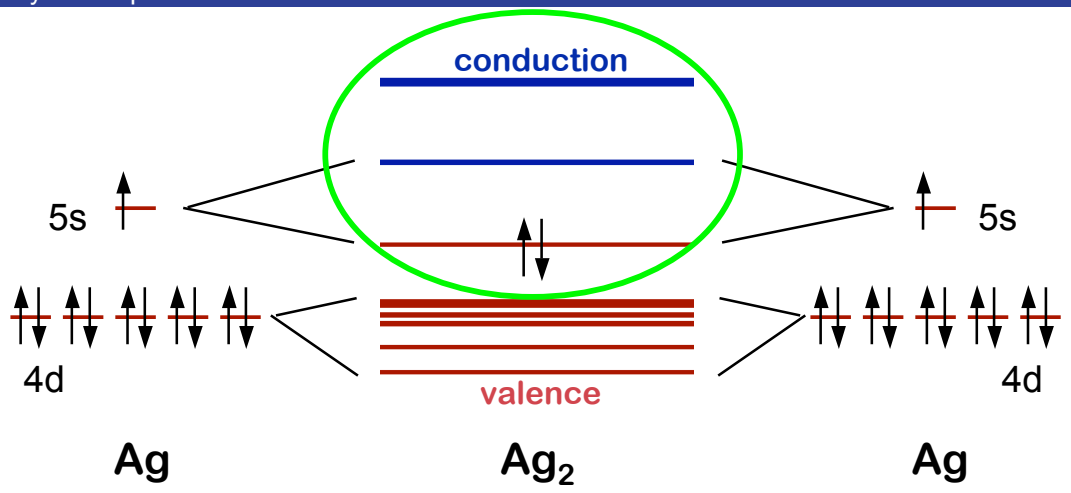

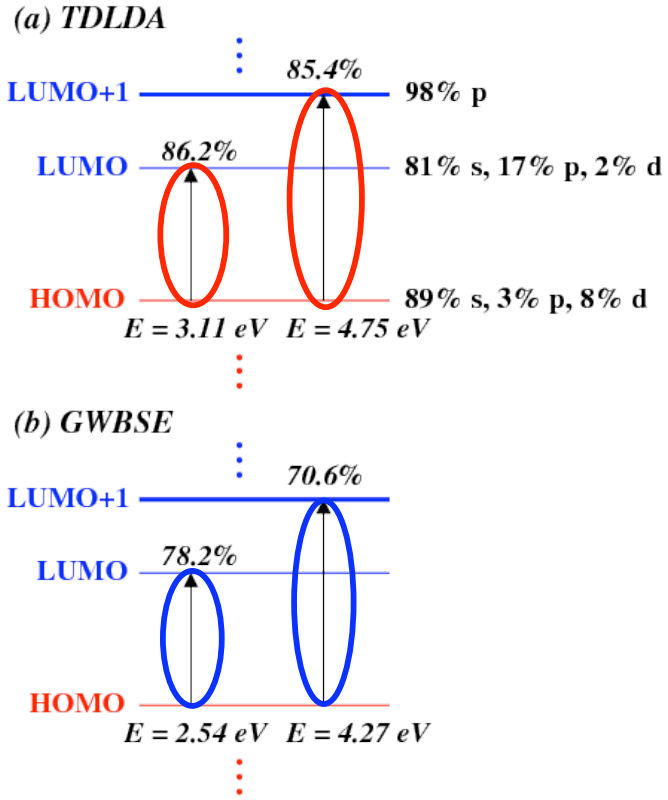

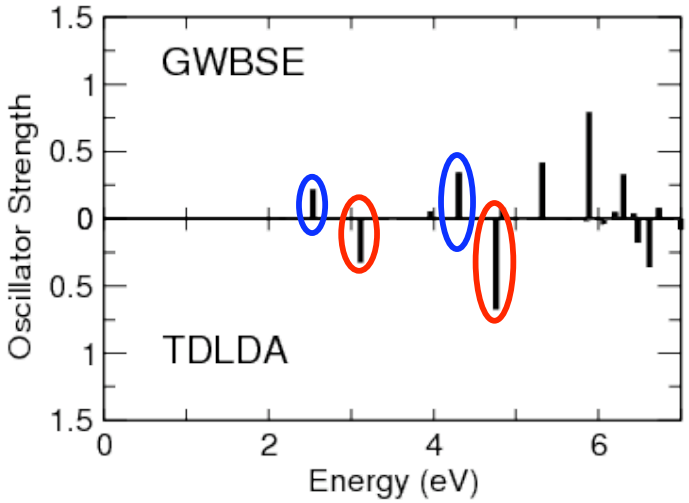

The increase in *d* character of optical excitations at the GWBSE level accompanied by a redshift and quenching of OS compared to TDLDA.

Thought experiment: "Remove" the *d* electrons

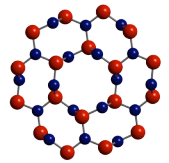

d : *v* = 1 - 10 *s*: *v* = 11 (HOMO)

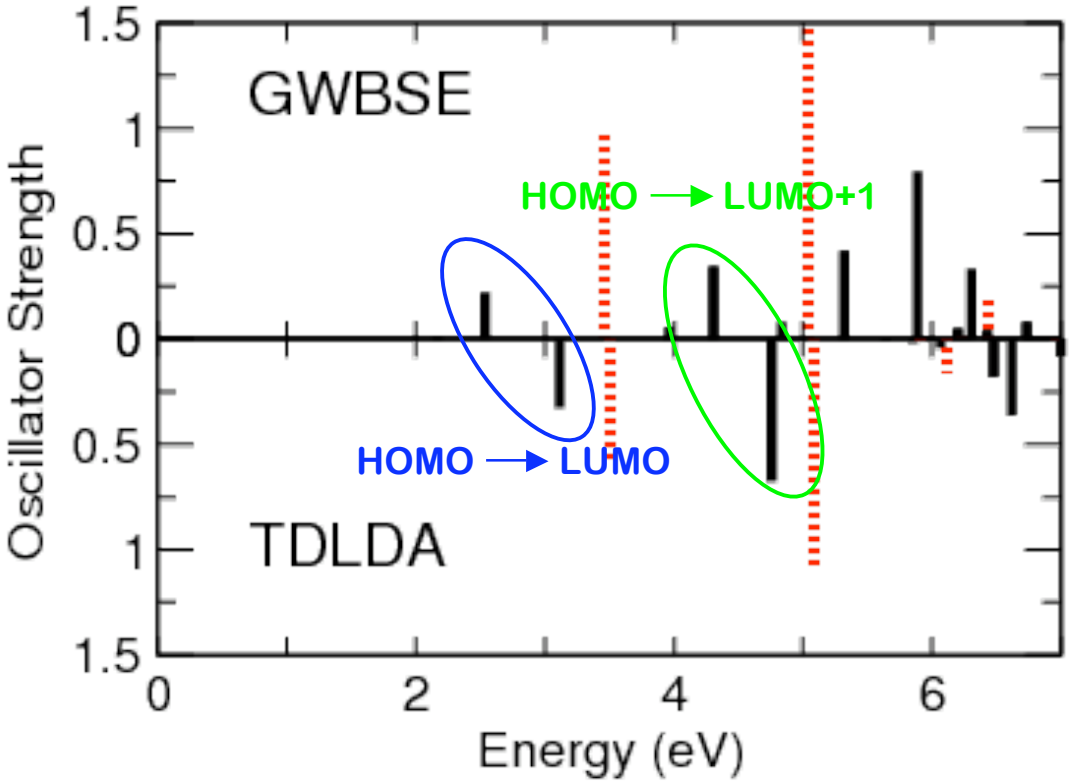

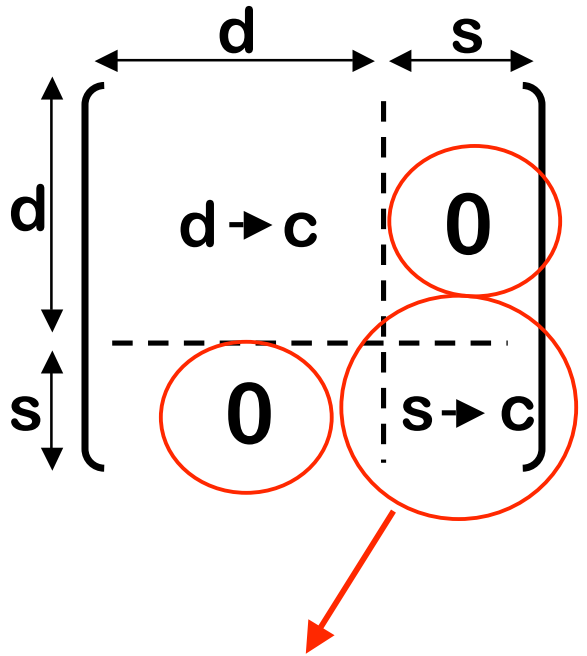

Diagonalize this only

When *d* electrons are removed, very good agreement between TDLDA and GWBSE.

From Nanocrystals to Nanoshells

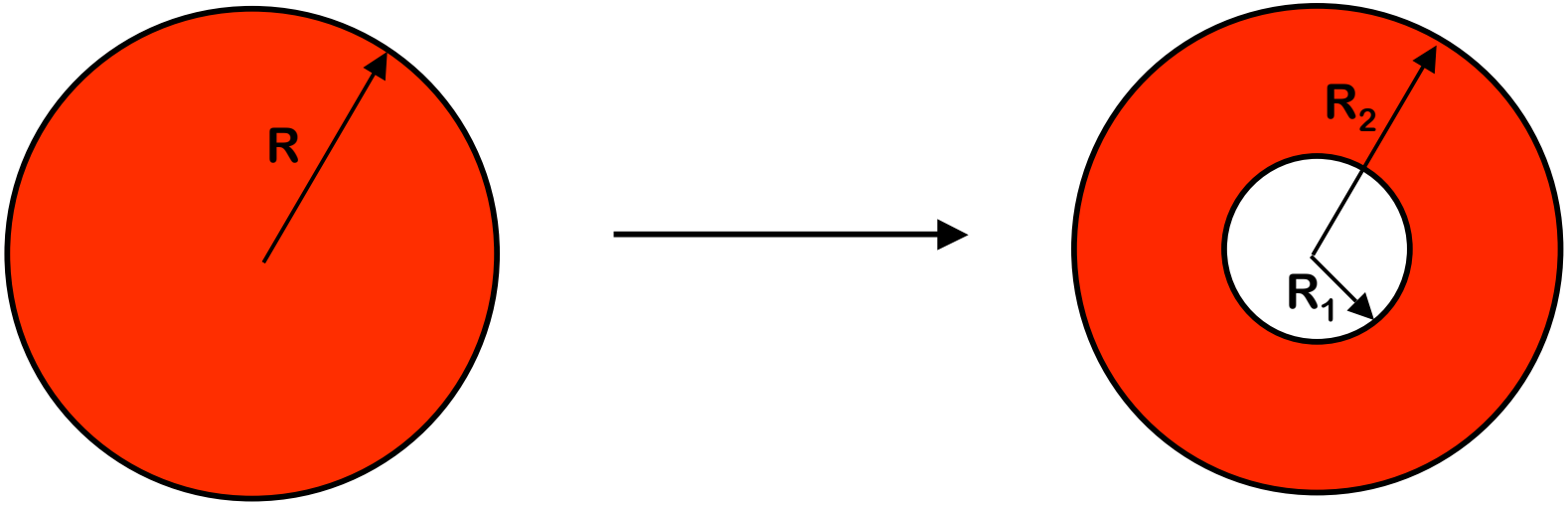

- How do electronic and optical properties of Si nanostructures evolve in going from quantum dots to “nanoshells”?
- Recent interest in optical properties of metallic (typically Au or Ag) shells over a dielectric core.
- Dielectric and optical properties of Si nanostructures are, in many ways, reminiscent of metallic nanoparticles, with the added bonus that Si is much easier to work with!
- Just got curious about effects of confinement vs geometry in Si nanostructures.

Predictions from Effective Mass Approximation

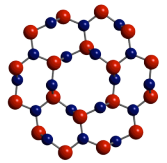

- **Single-band effective mass approximation (EMA) for impenetrable nanoshells**

$$V(r) = 0 \quad \text{if} \quad R_1 < r < R_2 \quad \text{and} \quad \infty \quad \text{elsewhere}$$

- **The *l = m = 0* eigen-functions are**

$$\psi(\vec{r}) = \frac{1}{\sqrt{2\pi(R_2 - R_1)}} \frac{\sin\left(\frac{\pi(R_2 - r)}{R_2 - R_1}\right)}{r} \quad \text{for} \quad R_1 < r < R_2$$

- **The energy spectrum *E* depends only on the thickness $t = R_2 - R_1$ implying $E_{gap}(R_1,R_2) = E_{gap}(t) \sim t^{-2}$**

- **To investigate the real R_1, R_2 dependence of Si nanoshells, considered**
  - **Nanoshells of fixed R_1 (changing R_2)**
  - **Nanoshells of fixed R_2 (changing R_1 from 0 to $R_{1,max}$)**

Both the inner and outer surfaces were passivated by H.

Computational Parameters, Methods, *GW* Test

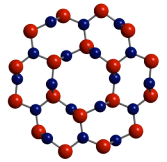

- ***Ab initio*** real-space calculations (PARSEC) with TM pseudopotentials using a grid spacing h = 0.6 a.u. and boundary radii from 36 a.u. to 50 a.u.

- Quasiparticle gaps calculated with ΔSCF method by computing ionization potentials (IP) and electron affinities (EA) of *n*-electron nanoshells:

$$IP = E(n-1) - E(n) \qquad EA = E(n) - E(n+1) \qquad E_{gap} = IP - EA$$

- ***GW*** calculations on Si quantum dots suggest that the ΔSCF method is accurate for EA, while IPs should be shifted upward by ~ 0.5 eV.
[Tiago and Chelikowsky, PRB 73, 205334 (2006)]

- Performed GW_f calculations on the smallest nanoshell $Si_{156}H_{184}$ (R_1 = 5 A , R_2 = 10.3 A) with h = 0.8 a.u., 750 orbitals (404 occupied). Self-energy computed with a vertex correction using the TDLDA polarizability

	ΔSCF	GW_f
IP (eV)	6.65	7.10
EA (eV)	2.62	2.56

Similar trend for Si nanoshells

Size Dependence of Quasiparticle Gaps

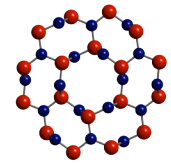

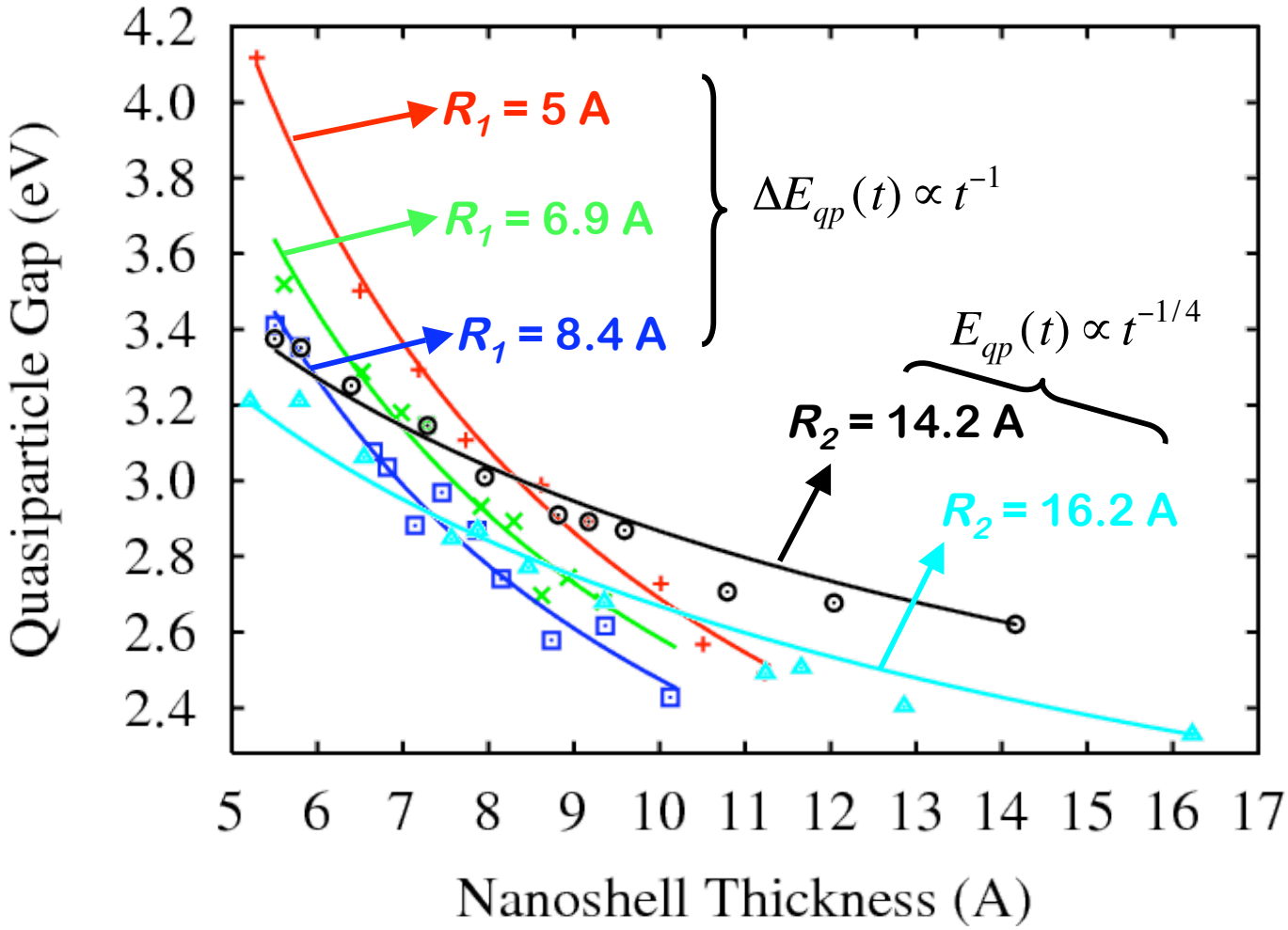

Exciton Coulomb Energies for Q. Dots

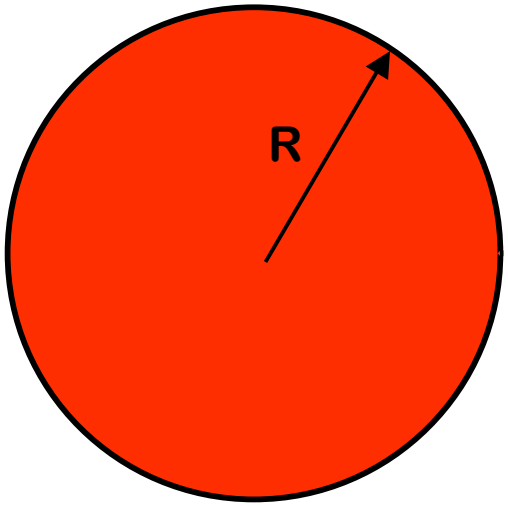

$$E_{Coul}(\varepsilon = 1) = \iint \frac{|\psi_e(\vec{r}_1)|^2 |\psi_h(\vec{r}_2)|^2}{|\vec{r}_1 - \vec{r}_2|} d^3\vec{r}_1 d^3\vec{r}_2$$

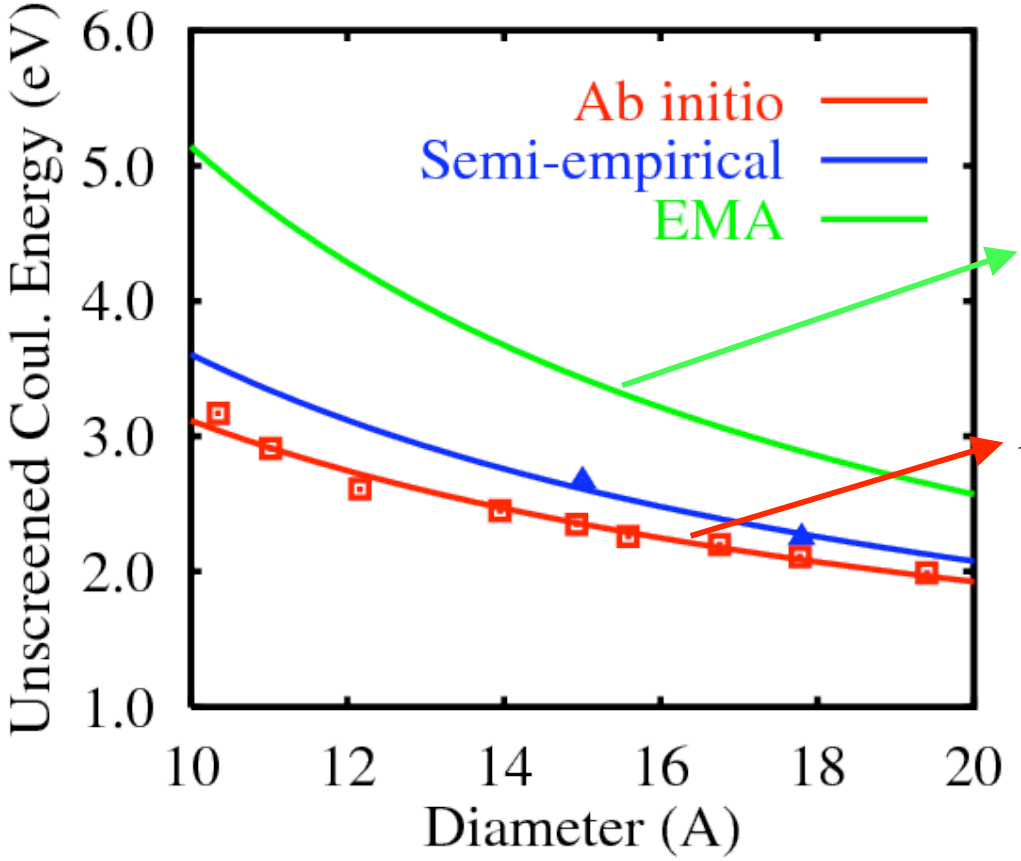

$$E_{Coul}^{EMA} = \frac{1.786}{R}$$

$$E_{Coul}^{Ab\ Initio} \propto R^{-0.7}$$

Exciton Coulomb Energies for Nanoshells

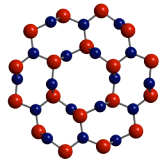

The unscreened Coulomb energy in the EMA with envelope wavefunctions vanishing at the inner/outer radii can be evaluated.

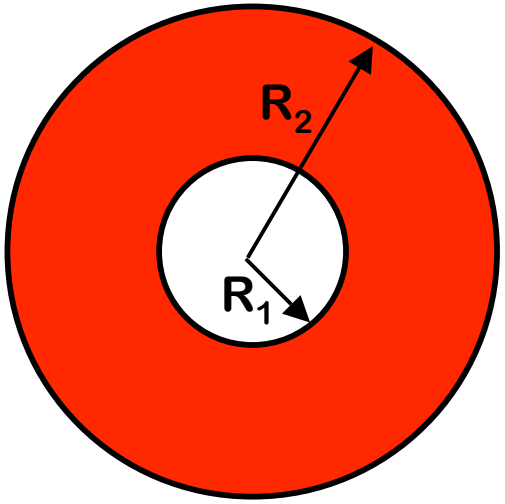

$t = R_2 - R_1$

$$E_{Coul} = \frac{2}{\pi t}\int_0^{\pi} dx \, \frac{\sin^2 x(2x - \sin 2x)}{x + \frac{\pi R_1}{t}}$$

$$\left(R_1 \to 0 \quad E_{Coul} = \frac{1.786}{t} \right)$$

Even at the EMA level, E_{Coul} depends on both R_1 and R_2

Exciton Coulomb Energies at Fixed R_1

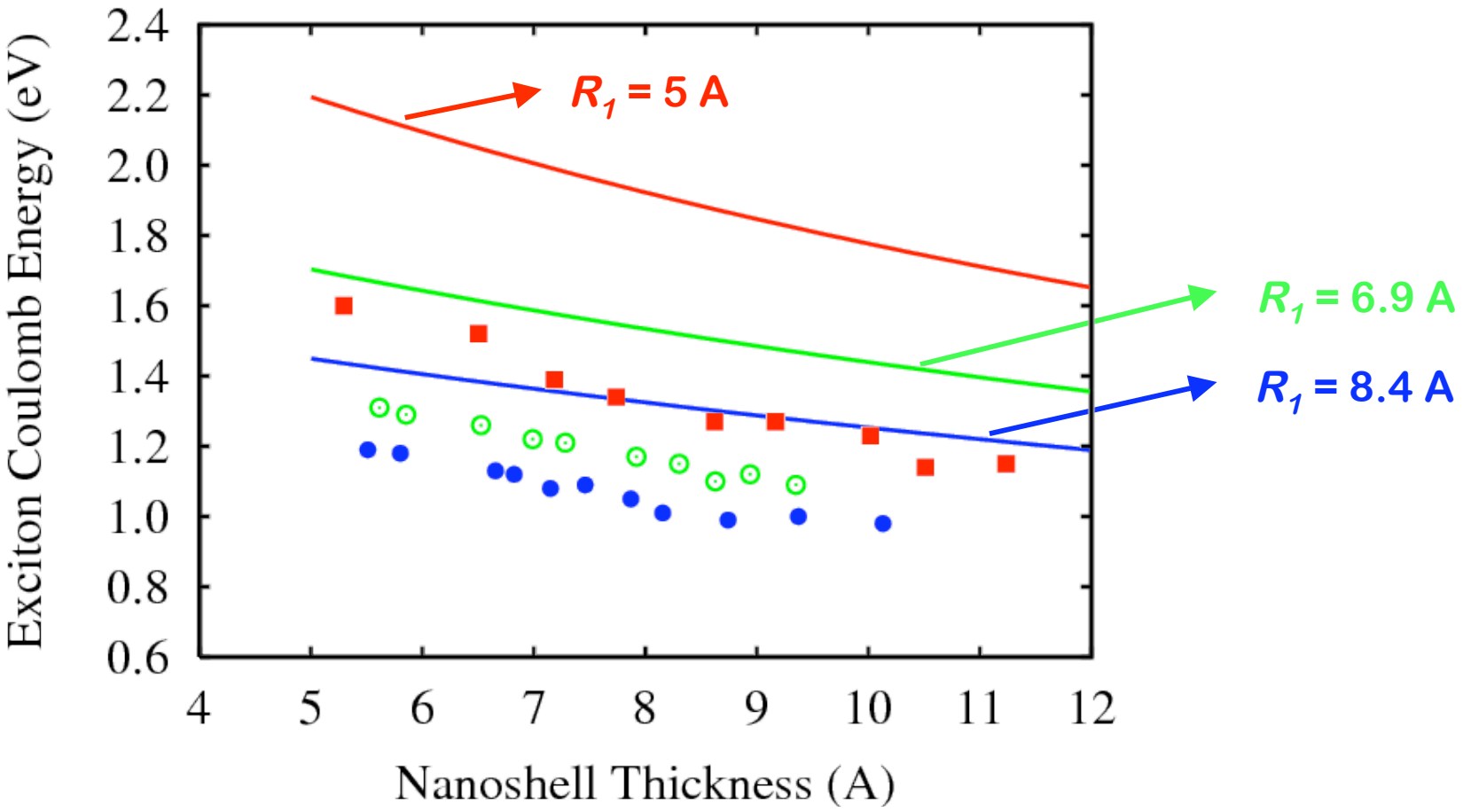

- Both EMA and *ab initio* results find an inverse correlation of E_{Coul} with nanoshell thickness at fixed R_1 (Quantum confinement).
- *Ab initio* results significantly reduced in magnitude wrt EMA predictions.

Exciton Coulomb Energies at Fixed R_2

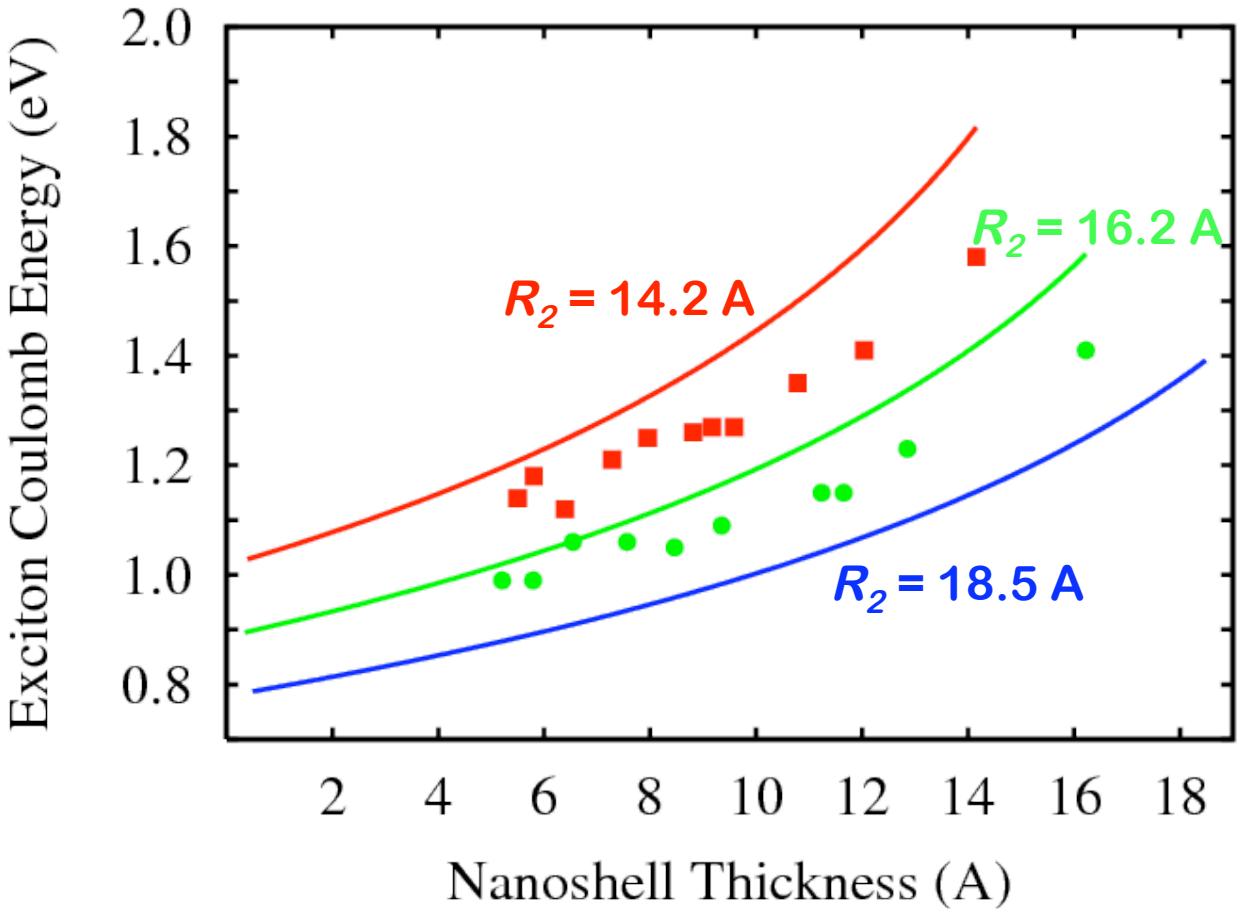

E_{Coul} *decreases* as the nanoshell becomes *more confining*!

Confinement versus Geometry

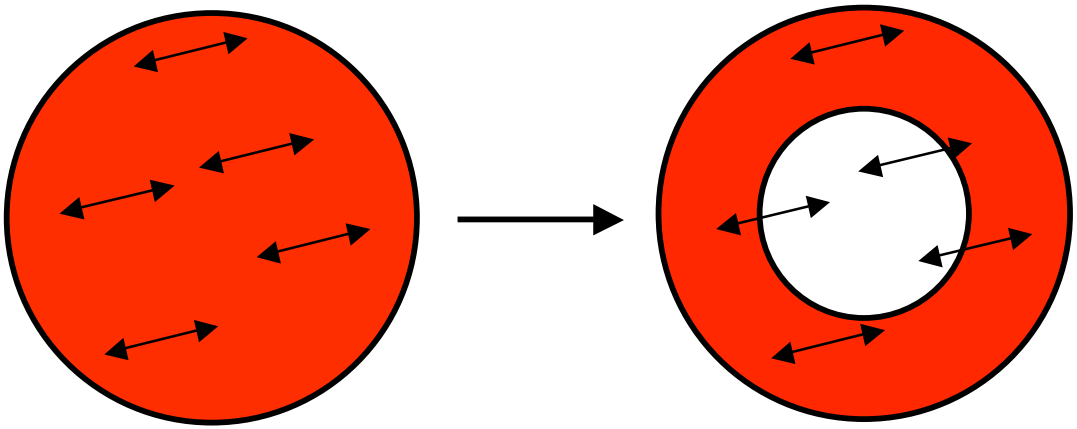

In going from the quantum dot to the nanoshell

- **The *e* or *h* "wavefunction amplitude" increases (confinement)**
- **The average distance between *e* and *h* increases (less Coulomb interaction)**

For a spherical shell, the distance "wins" ⇒ less E_{Coul}

Easiest way to see this: Assume a somewhat unrealistic "constant" wavefunction for the *e* or the *h*. E_{Coul} can be calculated analytically

$$\psi(\vec{r}) = V^{-1/2} \quad \Rightarrow \quad E_{Coul}(R_1 \neq 0, R_2) < E_{Coul}(R_1 = 0, R_2)$$

Topology versus Geometry

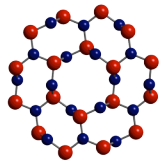

The nanoshell is neither convex (geometrical) nor simple-connected (topological).

Which is more important?

How about the case of a nano-star or a nano-crescent-moon?
Simple-connected yet non-convex

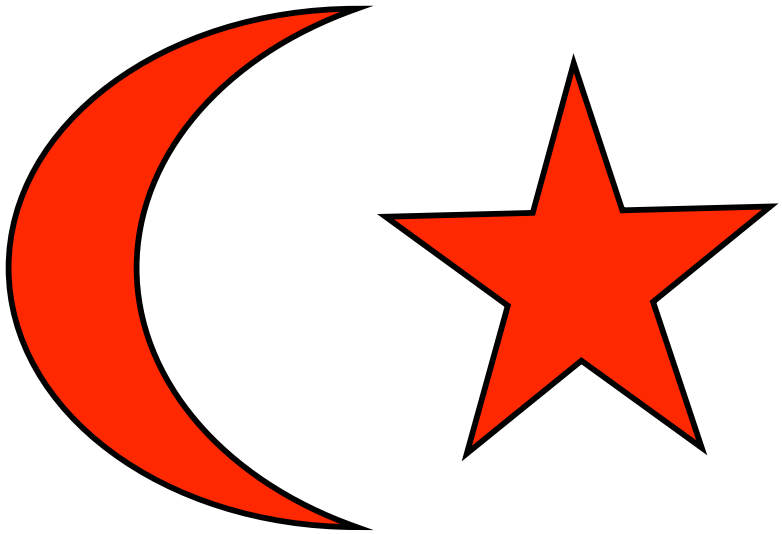

Summary

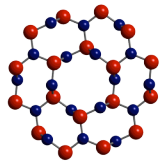

- Time-dependent density functional theory (TDDFT) within the local density approximation (TDLDA) generally yields good agreement with existing experimental studies on absorption spectra of noble Ag_n (n = 1 - 20) clusters.

- *d* electrons affect optical spectra in two distinct ways: (i) quenching the oscillator strengths by screening the *s* electrons, and (ii) by getting directly involved in low-energy optical excitations. These effects enhance in going from Ag to Au to Cu due to increased *spd* hybridization.

- Many-body approach based on the solution of the Bethe-Salpeter equation for the two-particle Green's function (GWBSE method) with standard (non-semicore) pseudopotentials has serious deficiencies (over-screening *s* electrons, strong non-locality) compared to TDDFT.

- The size dependence of electronic excitations in a Si nanoshell can be explained quite well, to a first approximation, by assuming it to be a metallic macroscopic object (within classical EM). Exciton Coulomb energies, on the other hand, have counter-intuitive (in the "nano" quantum-confinement-sense) size dependencies.

- Nano is not just "small". Geometry (or topology) is just as important as "small"